Analysis of Long-term Ex-vessel Debris Coolability with a Simple Model

Byoungcheol Hwang [a], Kiyofumi Moriyama [a], Hyun Sun Park [a*]
[a]*Division of Advanced Nuclear Engineering, POSTECH, Hyoja-dong, Nam-gu, Pohang, Kyung-buk, South Korea*
[*]Corresponding author: hejsunny@postech.ac.kr

1. Introduction

In the late phase of the severe accident in light water reactors (LWRs), assuring the coolability of ex-vessel core debris is important because it is the last barrier to prevent the accident progression before the radioactive release to the environment. If the debris cooling is unsuccessful, the heated and possibly re-melted core debris may induces molten core-concrete interaction (MCCI) that produces steam and non-condensable gases and causes the over-pressurization of containment vessel. Analysis for the long-term cooling of an ex-vessel debris bed was performed using a simple model developed by Hwang et al. [1], and the model was originally developed to explain the feature of the debris bed in FARO experiments [2]. It is assumed that the debris bed consists of a fluidized particles on top and a porous lump of sintered particles below. The bed formation process is also considered to determine the geometry and initial condition of the debris bed. Therefore, the simple model includes a wide range of cooling processes with a simplified zero or one-dimensional analysis. In this research, additional models including the consideration of the decay heat and an empirical model for debris size distribution were added and the modified model was applied to a plant scale condition, APR1400. We examined the impact of input variables including 10 initial/boundary condition variables and 5 model parameters with 23 test cases in total, calculated up to 50 hours after debris bed formation. The results showed that smaller areas of debris bed accumulation cause higher maximum temperatures of debris bed, and large jet diameter, shallow coolant depth, and large jet breakup constant also have influence on the long-term cooling.

2. Methods and Results

The analytical model developed by Hwang et al. [1] was modified for the plant scale sensitivity tests. The original model [1] simulated the FARO experiments [2] and it showed a good agreement. Section 2.1 shows the brief description of original model and modifications: geometrical information, porosity model of loose particle, decay heat model, and particle size distribution model. Section 2.2 describes the characteristics of input parameters, and the results are shown in Section 2.3 ~ 2.5.

2.1 Analytical Model

The ex-vessel cooling scenario in the original model is divided into three parts: particle falling period, bed formation period, and long-term cooling period as shown in Fig. 1. In the particle falling period ('A' in Fig. 1), the falling time of fragmented particles (0.4 ~ 15mm) is calculated using the force balance between buoyancy, drag, and gravity force. Also, the effect of vapor velocity caused by the fuel coolant interaction (FCI) is considered. Using this time data, the variation of enthalpy during particle falling is calculated, so we can decide whether the particle is re-melted or solid state at cavity bottom ('B' in Fig. 1). The re-melted corium, i.e. larger particles, wicks into the pore of the particulate debris bed, then finally forms a 'cake', a lump of sintered particles. The 'cake' and the 'loose particle' (the upper particle region in debris bed) go through the long-term cooling period ('C' in Fig. 1). As a limitation of a one-dimensional model, the heat release from the debris bed occurs only at the top and bottom.

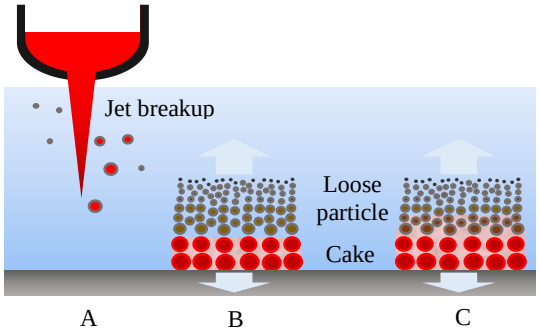

Fig. 1. Schematic diagram for ex-vessel scenario : A (particle falling period), B (bed formation period), C (long-term cooling period)

The additional models are as follows. First, the geometry and material for APR1400 was applied (cavity depth about 6.6m, the floor material siliceous concrete [3]). Second, the porosity of the debris bed (loose particle and cake) was assumed to 0.5 in the original Hwang's model. However, the porosity of the cake should be smaller than the loose particle due to t sintering, and this effect is considered. Third, we implemented the a correlation for the decay heat [4],

$$\frac{P(t_s)}{P_0} = 1.250 \times 10^{-1} \times t_s^{-0.2752} \quad (\text{for } 10^2 \le t_s \le 10^6)$$

where P_0 is the operation power for an infinite period before shutdown (about 4200 MWth for ARP1400), t_s is the time after shutdown. The effect of decay heat is considered only for the long-term cooling period because the initial superheat is dominant in the particle falling and the debris bed formation periods. Finally, the size

distribution of particles was considered by an empirical correlation [5] using the Rosin-Rammler distribution,

$$F = 1 - \exp\left\{-\left(\frac{D_p}{D_e}\right)^{n}\right\}$$
$$\mathrm{D_e} = \frac{D_{MM}}{(log2)^{\frac{1}{n}}}\ , \qquad n = 1.5$$

where F is the cumulative mass fraction of particles smaller than a diameter, D_p, D_{MM} is the mass median diameter, D_e is the absolute size constant, and n is the distribution constant.

2.2 Initial/Boundary conditions and model parameters

A sensitivity analysis was performed on 15 input variables composed of 10 initial/boundary conditions (water temperature [6, 7], jet diameter [8], jet velocity [9], water depth [9], melt initial temperature [10], melt mass [6], porosity [11], accumulation area [12], time duration after shutdown [13], and loose particle thermal conductivity [1]) and 5 model parameters (jet breakup constant, vapor velocity constant, view factor, sintering effect constant, and particle size constant).The base case condition and range of the variables for the sensitivity study is indicated in Table I. The cases are, hereafter, called by the abbreviated names in the table for convenience.

Table I: Input variables and ranges for sensitivity analysis

Parameter	Range	Basecase	Abbr.
Water temperature [K]	300 ~ 350	300	WT
Jet diameter [m]	0.2 ~ 0.28	0.2	JD
Jet velocity [m/s]	6 ~ 12	6	JV
Water depth [m]	3.5 ~ 5.6	5.6	WD
Melt initial temperature [K]	2900 ~ 3400	3150	MT
Melt mass [t]	120 ~ 145	145	MM
Porosity	0.3 ~ 0.6	0.45	PO
Accumulation area [m^2]	21 ~ 84	42	AA
Duration after shutdown [hr]	2 ~ 20	2	TAU
Loose particle conductivity [W/mk]	30 ~ 250	30	KLP
Jet breakup constant	0.5 ~ 0.9	0.7	CJB
Vapor velocity constant	172.3 ~ 220.6	172.3	CV
View factor	0.1 ~ 0.5	0.3	VF
Sintering effect constant	5 ~ 20	12	CS
Particle size constant	1.428 ~ 0.572	1	CD

2.3 Sensitivity results I: particle falling period

In the particle falling period, impacts of 5 parameters (jet diameter (JD), jet inlet velocity (JV), water depth (WD), jet breakup constant (CJB), and particle velocity constant (CV)) were examined. The letter 'H' is added for the cases with higher values than the base case (JDH, JVH, CJBH) and 'L' is for lower values (CVL, WDL1, WDL2, CJBL). The case WDL1 is the case with 4.5m water depth and WDL2 is with 3.5m, a more severe condition.

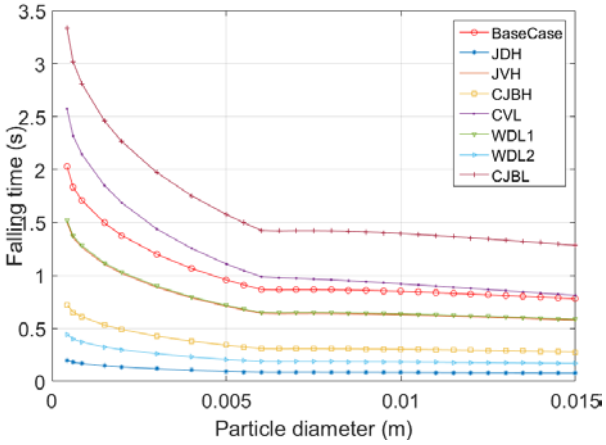

Fig. 2. Particle falling time according to particle size for each input parameter

Fig. 2 shows the comparison of the particle falling time depending on the particle size, and it shows that the curve changes at 0.006m because the flow regime changes. The effects of the jet breakup constant (CJBH, CJBL) and jet diameter (JDH) were very strong, and the water depth (WDL1, WDL2) also showed strong impacts. However, the effect of particle velocity constant (CVL) was weak.

2.4 Sensitivity results II: bed formation period

In the debris bed formation period, 5 more parameters (water temperature (WT), initial melt temperature (MT), view factor (VF), sintering effect constant (CS), particle size constant (CD)) were examined. The result parameter is 'normalized excess specific enthalpy' which is defined by the ratio of the volume average particle enthalpy to the enthalpy for solidification, and serves as the criterion of re-melting, and shown in Fig. 3 The values larger than unity mean that the particle is re-melted at the pool bottom. The base case has a small amount of melting region (particles larger than about 14mm). In cases of larger jet diameter (JDH), larger jet breakup constant (CJBH), and smaller water depth (WDL2), even smaller particles were also re-melted. The trend in the cases of varied melt initial temperatures (MTH, MTL) was

similar to the base case in the smaller particle region, but different to some extent for larger particle sizes.

The cake mass fraction was calculated based on the sintering concept. The effects of sintering constant (CSH, CSL) and particle size distribution (CDH, CDL) were also considered and Table II shows the cake fraction corresponding to the variation of input parameters. The base case shows 1.22% cake among total mass, and the whole part is cake for the condition of large jet diameter (JDH), strong vapor velocity effect (CJBH), and shallow water depth (WDL2). Also, the case for large fraction of smaller particles (CDH), lower initial melt temperature (MTL), and smaller jet breakup constant (CJBL) shows only loose particles formation without cake.

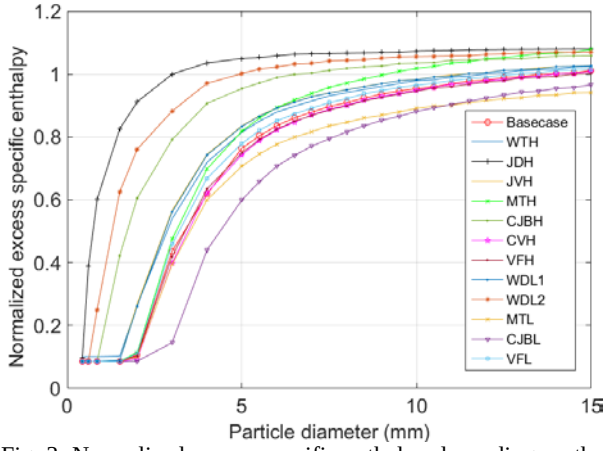

Fig. 3. Normalized excess specific enthalpy depending on the particle size and impacts for the variation of input parameters

Table II: Cake fraction corresponding to the variation of input parameters

Case	Base	WTH	JDH
Cake fraction (%)	1.22	2.48	100

JVH	MTH	CJBH	CVH	VFH
9.53	3.45	100	1.22	0.672

CSH	CDH	WDL1	WDL2	MTL
2.04	0.02	9.53	100	0.00

CJBL	VFL	CSL	CDL
0.00	3.09	0.51	28.7

2.5 Sensitivity results: long-term cooling period

After the formation of loose particle and cake, the calculation for 50 hours of long term cooling was performed for each case. Impacts of all the 15 parameters were examined in the results in this period. Fig. 4 shows the spatial temperature distribution (top) and history of temperature (bottom) for the base case. In spatial distribution, the region for x < 0m is the concrete side, a thin layer in the x > 0m region is the cake, and the rest of the part is the loose particle bed. The figure shows that the maximum temperature of loose particle region increases for 30min ~ 1hr. The temperature of the concrete surface is higher than debris bed parts at final time (50hrs) because of very low thermal conductivity in siliceous concrete. In the figure of temperature history (Fig. 4, bottom), the timing of temperature rising was different in the cake and loose particle regions.

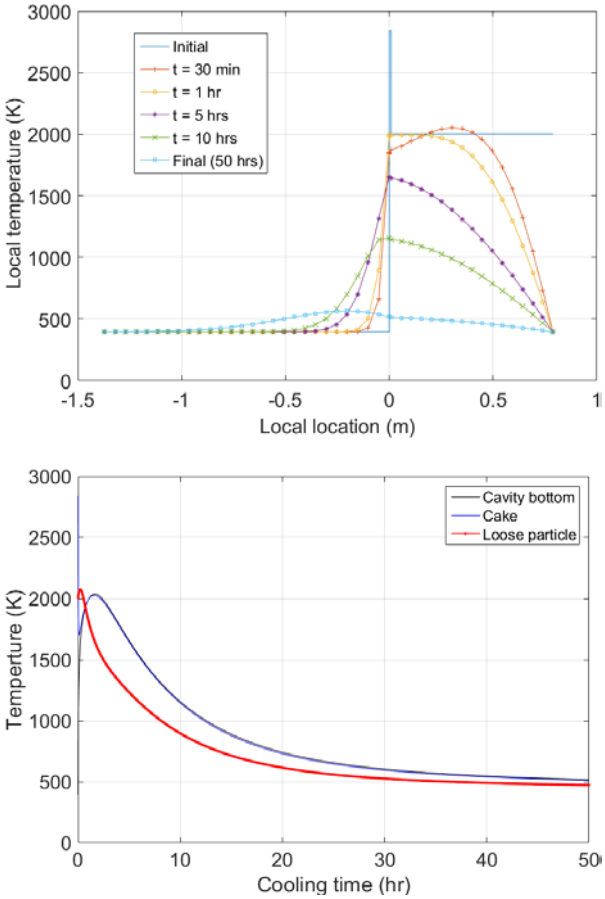

Fig. 4. Spatial temperature distribution (top) and history of the temperatures (bottom surface, centers of the cake and loose debris) (bottom) for the base case

The result parameter for long-term cooling period is the 'maximum temperature' in the debris bed at 50 hr. Fig. 5 shows the maximum temperature values for (a) the variation of initial/boundary condition variables and (b) the variation of model parameters. Among the initial/boundary condition variations, the cases for large jet diameter (JDH), shallow water depth (WDL2), and small accumulation area (AAL) show very high temperature compared to the base case. Also, the high initial melt temperature (MTH) case shows relatively high maximum temperature. The variation of other input parameters barely affects the result. In Fig.5 (b), the large jet breakup constant (CJBH) case shows the high value. The values of particle size constant (CDH, CDL) and sintering effect constant (CSL) are 100~200 K higher than the base case temperature.

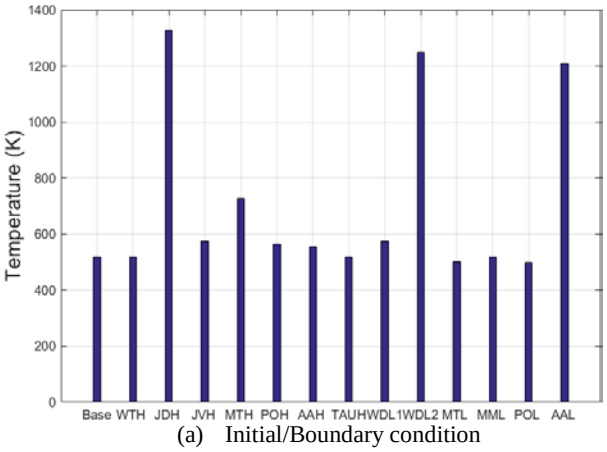

(a) Initial/Boundary condition

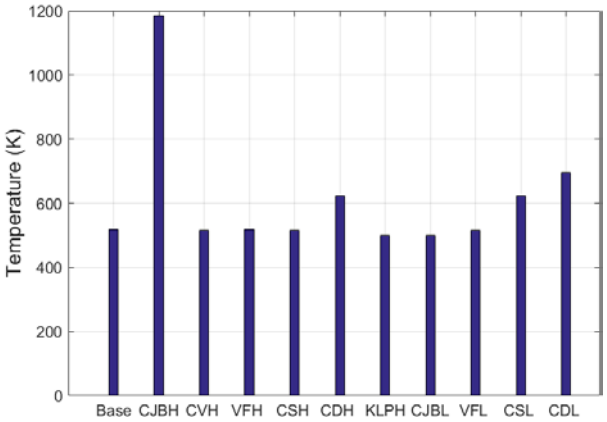

(b) Model parameters

Fig. 5. Comparison of the impact of input variables on the maximum temperature at 50 hours

3. Conclusions

Sensitivity tests for the ex-vessel debris bed cooling behavior on selected input variables were performed using a modified version of a simple model developed by Hwang et al. [1]. The model covers the series of phenomena from the breakup of the melt jet till the long-term cooling phase, and the results showed that the accumulation area of debris bed has significant impacts on the overall cooling performance. Also, the geometrical effect related to the jet breakup length and water pool depth dominates the cake formation.

ACKNOWLEDGEMENT

This work was supported by the Nuclear Safety Research Program through the Korea Foundation Of Nuclear Safety (KOFONS), granted financial resource from the Nuclear Safety and Security Commission (NSSC), Republic of Korea (No. 1305008). The authors thank professor Massoud Kaviany at University of Michigan and professor Gisuk Hwang at Wichita State University for technical support, and also thank Eunho Kim, and Mooneon Lee at Pohang University of Science and Technology (POSTECH) for code development.

REFERENCES

[1] G. Hwang et al., FARO tests corium-melt cooling in water pool: roles of melt superheat and sintering in sediment, Nuclear Engineering and Design, 2016 (Submitted).
[2] D. Magallon, Characteristics of corium debris bed generated in large-scale fuel-coolant interaction experiments, Nuclear Engineering and Design, Vol. 236, pp. 1998-2009, 2006.
[3] T, Sevon, Molten Core Concrete Interactions in Nuclear Accidents, VIT research note 2311, ESPOO, 2005.
[4] N. E. Todreas, M. S. Kazimi, Nuclear systems I: thermal hydraulic fundamentals, Taylor & Francis, 2012.
[5] K. Moriyama, Y. Maruyama, T. Usami, and H. Nakamura, Coarse break-up of a stream of oxide and steel melt in a water pool, JAERI-Research 2005-017, Japan Atomic Energy Research Institute, 2005.
[6] K. I. Ahn, S. H. Park, H. D. Kim, H. S. Park, The plant-specific uncertainty analysis for an ex-vessel steam explosion-induced pressure load using a TEXAS-SAUNA coupled system, Nuclear Engineering and Design, Vol. 249, pp. 400-412, 2012.
[7] J. H. Park, H. Y. Kim, S. W. Hong, K. S. Ha, MCCI simulation for the APR-1400 TLOFW sequence. Trans. the Korean Nuclear Society (2011 Spring Meeting), Taebaek, 2011.
[8] R. Sairanen, G. Berthoud, G. Ratel, R. Meignen, H. Jacobs, M. Buerger, M. Buck, M. Moriyama, M. Naito, and J. Song, "OECD research programme on fuel−coolant interaction steam explosion resolution for nuclear applications", SERENA. Final Report, OECD/NEA, CSNI, Le Seine Saint-Germain, 12 boulevard des Iles, F-92130 Issy-les-Moulineaux (France), 2007.
[9] K. Moriyama, H. S. Park, Simulation of Ex-Vessel Melt Jet Breakup and Sensitivity on Model Parameters and Accident Conditions, NURETH16, Chicago (USA), Aug 30- Sep 4, 2015.
[10] OECD/NEA, OECD research program on fuel-coolant interaction: steam explosion resolution for nuclear applications-SERENA, final report, NEA/CSNI/R(2007)11, OECD/NEA/CSNI, 2007.
[11] T. N. Dinh, W. M. Ma, A. Karbojian, P. Kudinov, C. T. Tran, C. R. Hansson, Ex-Vessel Corium Coolability and Steam Explosion Energetics in Nordic Light Water Reactors, NKS-160, KTH (Sweden), 2008.
[12] KEPCO & KHNP Co. Ltd., Severe Accident Analysis Report, APR1400-E-P-NR-14003-NP, Rev.0, 2014.
[13] I. Ye, J. A. Kim, C. Ryu, K. S. Ha, H. Y. Kim, J. Song, Numerical investigation of the spreading and heat transfer characteristics of ex-vessel core melt, Nuclear Engineering Technology, Vol. 45, No. 1, 2012.